Photo-Initiated Polymerization of Liquid Crystalline Thiol-Ene Monomers in Isotropic and Anisotropic Solvents

Hans T. A. Wilderbeek,*,†,‡ Mark G. M. van der Meer,†,§ Cees W. M. Bastiaansen,†,‡ and Dirk J. Broer†,§

Eindhoven University of Technology, P.O. Box 513, 5600 MB Eindhoven, The Netherlands, Dutch Polymer Institute, P.O. Box 902, 5600 AX Eindhoven, The Netherlands, and Philips Research Laboratories, Professor Holstlaan 4, 5656 AA Eindhoven, The Netherlands

Received: July 1, 2002; In Final Form: September 19, 2002

We report on the photoinitiated polymerization of phenyl benzoate-based liquid crystalline (LC) thiol-ene monomers in isotropic and anisotropic solvents. The mixing behavior of the thiol-ene monomers with anisotropic cyanobiphenyl solvents was investigated, and unique reactive LC mixtures are formed that exhibit variable mesophases at ambient temperatures. Using size exclusion chromatography, the conversion of the thiol-ene monomers was studied in isotropic solvents and in anisotropic solvents as a function of several parameters, such as the irradiation time, polymerization temperature, and monomer concentration. Indications for the existence of a polymerization ceiling temperature effect were observed which was more pronounced for lower initial monomer concentrations. The in situ photopolymerization of the LC thiol-ene monomers in anisotropic media leads to a variety of morphological structures, ranging from intriguing threadlike architectures to dendritic crystalline structures. The morphological changes that occur during the polymerization process are complex, and several approaches toward the enhanced control over the resulting morphologies are discussed. The results and insights presented here could potentially lead to new architectures and enhanced optical and electrooptical properties of devices.

Introduction

The dominant position of liquid crystal displays (LCDs) as a man−machine interface has been firmly established in present-day society, despite the progress in alternative technologies such as polymer light emitting diodes[1] and electrochromic displays.[2] Over the past few years, polymer-stabilized liquid crystal (LC) effects have been investigated with the aim of further optimizing LCDs. Such polymer/liquid crystal composites have hitherto always consisted of combinations of low molecular weight liquid crystals and flexible polymers,[3] dispersed polymer particles,[4] side-chain liquid crystal polymers,[5] or isotropic or anisotropic network-type structures.[6−10] The order parameter associated with the mesogenic moieties in conventional side-chain and network-type systems is comparable to the order parameter of low molar mass liquid crystals, however, and is limited to a maximum of approximately 0.7. Although rotational mobility is hindered, a higher order parameter should in principle be possible but is limited by the steric hindrance caused by the polymer backbone. This hinders perfect alignment of the mesogenic core, despite the decoupling of the core from the polymer backbone. Other parts of the molecule are ordered to an even lesser extent. The alkylene spacer that is generally used has an order parameter of approximately 0.4, whereas the polymer chain shows hardly any order at all.[11] As a consequence, it is only the mesogenic units in the polymer network that provide the internal director field, which forms the driving force for relaxation to the aligned state if no external field conditions are present.

In the case of *main-chain* polymers, it is anticipated that the whole molecule will be aligned to a high degree of order, resulting from the larger aspect ratio,[12,13] thus giving rise to a higher degree of orientation in comparison to the side-chain and network-type structures. An enhanced optical performance (e.g., contrast ratio, faster relaxation) can therefore be realized, potentially leading to fast nematic switches, stabilized ferroelectrics, or switchable gratings, for instance, depending on the actual morphology of the polymer/LC composite on a nanoscale or microscale (Figure 1).

Up until now, the only reported structures similar to the main-chain polymer/LC systems described here were based on reversible, noncovalently linked building blocks dispersed in anisotropic solvents.[14−16] However, the polymerization process that involves the generation of covalent bonds has a significant advantage over the reversible noncovalent structures: it can be initiated on demand at a fixed temperature, using UV-irradiation, for example. This also introduces the possibility of the formation of the polymeric structures at specified positions, for example, through patterning processes or holographic approaches, thus further extending the control over the final morphology. These features cannot be accomplished using the reversible, noncovalently based systems where the supramolecular organization is obtained immediately and uniformly upon mixing the components in question.

To create the proposed covalently linked systems, materials must be available that enable the generation of such linear polymeric architectures. Monomers containing mercapto and vinyl groups, i.e., thiol-ene monomers, can be polymerized via a free-radical propagated step-growth mechanism,[17] leading to

* To whom correspondence should be addressed. Present address: Philips Research Laboratories, Professor Holstlaan 4, 5656 AA Eindhoven, The Netherlands. E-mail: hans.wilderbeek@philips.com.
† Eindhoven University of Technology.
‡ Dutch Polymer Institute.
§ Philips Research Laboratories.

10.1021/jp0215419 CCC: $22.00
Published on Web 11/23/2002

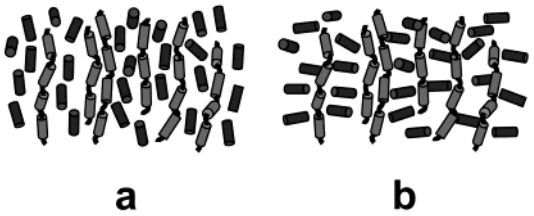

Figure 1. Schematic representation of main-chain liquid crystalline structures in a low molecular weight LC matrix. Depending on the dielectric properties of the matrix material and the external field conditions, a homeotropic (a) or a planar configuration (b) of the low molecular weight component is conceivable.

SCHEME 1: Simplified Schematic Overview of the Photo-Initiated Thiol-ene Free-Radical Polymerization Mechanism[a]

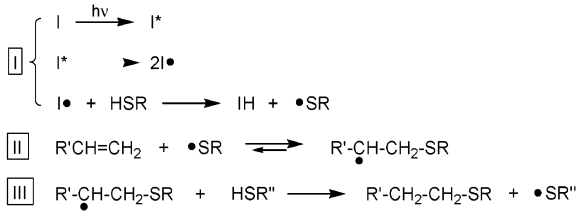

[a] (I) Initiation. (II) Thiol-ene addition Reaction. (III) Propagation.

the desired main-chain polymers (Scheme 1). Monomers containing a thiol functionality also benefit from having specific thiol-substrate interactions, for instance, which provide an additional means of morphology control through the patterned alignment of liquid crystals.[18] Alternatively, LC thiol-ene polymers can be created using dithiols and dienes (e.g., diacrylates).[19] However, monomers containing both functional groups benefit from having a theoretically required intrinsic 1:1 thiol-ene stoechiometry.

Liquid crystalline thiol-ene monomers have been reported before,[12,13,20] but their use was directed toward bulk polymerization. Here, we have designed novel polymer/LC systems based on the in situ polymerization of an initially homogeneous mixture of a mesogenic thiol-ene monomer and an inert anisotropic solvent. To generate homogeneous mixtures of monomer and solvent at ambient temperatures, liquid crystalline thiol-ene monomers with low melting temperatures are required. Yet, the reported liquid crystalline thiol-ene monomers display high transition temperatures originating from their bulky rigid core, despite the attempt to lower the transitions by introducing asymmetry through a methyl substituent. A single compound with a smaller mesogenic group based on a double phenyl core was shown to exhibit lower temperatures[12] and therefore formed an ideal template for further synthesis of other homologues (Table 1).[21] The photoinitiated bulk polymerization of these homologues and the analysis of the corresponding liquid crystalline thiol-ene polymers were described previously.[22]

In this paper, we describe the photoinitiated polymerization of these thiol-ene monomers in isotropic and anisotropic media. The mixing behavior of the liquid crystalline thiol-ene monomers with commercially available solvents is described, and the polymerization kinetics are investigated. New routes are also explored to grow these main-chain polymeric structures in the anisotropic media and to control the resulting morphology by spontaneous and/or enforced molecular organization.

Experimental Section

Materials. The liquid crystalline thiol-ene monomers **ThE 4b4**, **ThE 6b4**, and **ThE 6b6** were synthesized according to previously reported procedures.[21,23] The liquid crystalline cyanobiphenyl solvents **6CB** [4-hexyl-(1,1-biphenyl)-4-carbonitrile; K18] and **8CB** [4-octyl-(1,1-biphenyl)-4-carbonitrile; K24], the isotropic solvents chloroform and benzene, and the inhibitor hydroquinone were supplied by Merck (Poole, England or Darmstadt, Germany). 4-Chloroanisole and α-methylnaphthalene were supplied by Fluka Chemie AG, Buchs, Switzerland. The photoinitiator Irgacure 651 (α,α-dimethoxydeoxybenzoin) was supplied by Ciba Specialty Chemicals, Basel, Switzerland. HPLC-grade chloroform was used as the eluent for the size exclusion chromatography and was supplied by Biosolve, Valkenswaard, The Netherlands. All commercially available materials were used as received.

TABLE 1: Structure, Nomenclature and Transitions (°C) of Phenyl Benzoate Based ThE mbn Homologues[21a]

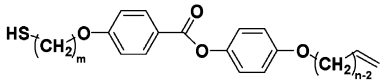

ThE mbn

structure	m	n	Cr	→	SmA	→	N	→	I
ThE 4b4	4	4		58.6				68.4	
ThE 5b4	5	4		60.6				72.8	
ThE 6b4	6	4		53.5		(48.3)		67.7	
ThE 6b6	6	6		42.5		55.4		69.5	

[a] Cr denotes the crystalline, SmA denotes the smectic A, N denotes the nematic, and I denotes the isotropic phase. The indices *m* and *n* refer to the number of carbon atoms in the spacers. Monotropic transitions are denoted in brackets.

Characterization Techniques. Phase diagrams were determined using both thermal characterization and optical microscopy. Thermal characterization was performed using a Perkin-Elmer Pyris1 differential scanning calorimeter (DSC) equipped with a CCA-7 temperature controller at a heating rate of 10 °C min^{-1}. The DSC was calibrated using indium, zinc, hexatriacontane, *n*-octane, and *n*-dodecane standards of high purity. Transition temperatures were determined using a Zeiss MC63 microscope with polarization optics, in combination with a Linkam THMS600 hot-stage. The samples were observed at heating rates not exceeding 1 °C min^{-1}, close to the actual transitions in order to determine the actual transition temperature.

Scanning electron microscopy (SEM) was performed using a Cambridge Stereoscan 2000 electron microscope. To study the morphology of samples confined between glass substrates ("cells") coated with an inert buffed polyimide alignment layer, an extraction method was performed first, analogous to procedures described elsewhere.[8,24] The low molecular weight components were extracted using *n*-hexane, a reasonable solvent for the cyanobiphenyls, but a nonsolvent for the thiol-ene polymers. The extracted cell was dried in a vacuum, carefully cleaved and coated with a thin gold/palladium alloy.

Wide-angle X-ray spectroscopy was performed at the European Synchrotron Radiation Facility (ESRF), Grenoble, France, using monochromatic X-rays with a wavelength $\lambda = 0.71795$ Å. Each diffraction pattern was recorded for 2−5 s on a two-dimensional Princeton CCD detector.

Size exclusion chromatography (SEC) of the monomers polymerized in isotropic media was performed using a Shimadzu LC-10AT liquid chromatograph equipped with a Polymer Laboratories Plgel 5μ 500 Å column in combination with a Linear UV−vis-205 absorbance detector ($\lambda = 254$ nm). SEC of the monomers polymerized in anisotropic media was performed using a Waters type 710B injector (50 μL) and two Polymer Labs, mixed-*d*, 7.8 × 300 mm columns thermostated

by a Spark Holland Mistral thermostat at 30 °C. The columns were calibrated using two mixtures of polystyrene calibration standards (Polymer Labs) in the range from 104 to 1 million g mol^{-1}. A Waters type 6000 pump provided a constant flow of 1 mL of chloroform min^{-1}. A Waters model 440 UV detector ($\lambda = 254$ and 263 nm) was used for detection. Samples were prepared by dissolution of the irradiated samples in 40 μL DSC sample pans in an exact known quantity of HPLC-grade chloroform to a concentration of approximately 0.1 mg mL^{-1}. A small amount of hydroquinone was added to prevent possible post-polymerization. Between 3 and 4 mL of these solutions were subsequently transferred into SEC-vials using a hypodermic syringe with a 2 μm filter. Provided the samples showed complete dissolution, based on a visual assessment, the conversion was determined by dividing the peak area of the residual monomer by the total peak area originating from the monomer, oligomeric and polymeric fractions, analogous to a previously reported procedure.[25] If a sample showed only partial dissolution, the conversion was based on the ratio between the residual monomer peak area and the peak area of a nonpolymerized reference sample. Peak-fitting routines were used to separate the monomer peak from the anisotropic solvent peak.

Polymer Synthesis. Photoinitiated polymerizations were carried out in small 30−50 μL aluminum DSC sample pans. The quantities, typically 6−13 mg for the anisotropic solvent experiments, were sufficiently small to ensure the formation of a small film of equal thickness in each case. The reflective aluminum substrate also functioned to level out possible UV-intensity gradients throughout the sample. The samples were irradiated using a Philips PL-S 10 UV-light source, connected to a timer at an approximate sample-light source distance of 10 cm. All irradiations were carried out in an inert argon environment. Polymerizations in isotropic solvents were performed in sealed flat glass slides (Camlab Ltd., Cambridge) with a known thickness in the range 0.3−2 mm. In all cases, the photoinitiator (Irgacure 651) content was 1% w/w, based on the monomer, unless stated otherwise.

Results and Discussion

Polymerization in Isotropic Solvents. Prior to the investigations of the polymerization behavior of thiol-ene monomers in anisotropic solvents, we conducted a brief intermediate feasibility study on the photopolymerization of these thiol-ene monomers in isotropic solvents. Unfortunately, the choice of isotropic solvent is less straightforward than may appear at first sight. The solubility of the thiol-ene monomers and polymers is low, which is not uncommon for main-chain liquid crystalline polymers, and only a few solvents were found that were able to dissolve the monomers and oligomers/polymers sufficiently, such as chloroform (or dichloromethane to a lesser extent), benzene, and the more exotic 4-chloroanisole, 1,1,2,2-tetrachloroethane, and hexafluoro-2-propanol. Figure 2 shows SEC chromatograms of **ThE 6b4**, containing 1% w/w photoinitiator, and in this particular case also containing a small amount of thioester with a 1:1 thiol-to-olefin ratio. Solutions of 5% w/w monomer in the selected isotropic solvents were photopolymerized at 25 °C for 15 min.

From the four isotropic solvents used, two solvents display a substantial degree of monomer conversion after a polymerization time of 15 min. In both chloroform and benzene, a decrease of the monomer signal is noticeable at the retention time of 546 s, along with the appearance of higher molecular weight fractions at shorter retention times (number average molecular weight $\bar{M}_n = 11.3$ kg mol^{-1} for chloroform, $\bar{M}_n =$ 6.9 kg mol^{-1} for benzene). 4-Chloroanisole is a poor solvent, which is reflected in the marginal polymerization of the monomer ($\bar{M}_n = 2.5$ kg mol^{-1}). α-Methylnaphthalene is a reasonable solvent for the monomer but has a strong UV-to-visible absorption, thus strongly limiting the degree of polymerization. Based on the obtained results, further experiments were carried out in chloroform; benzene was rejected because of its higher toxicity.

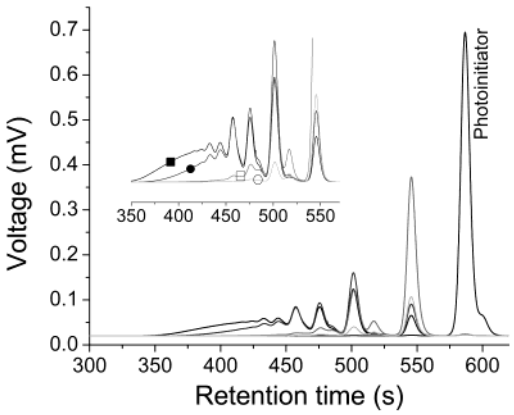

Figure 2. Size exclusion chromatogram of 5% w/w **ThE 6b4**, photopolymerized for 15 min at 25 °C in chloroform (■), benzene (●), 4-chloroanisole (□), and α−methylnaphthalene (○). The inset shows a magnification of the main graph.

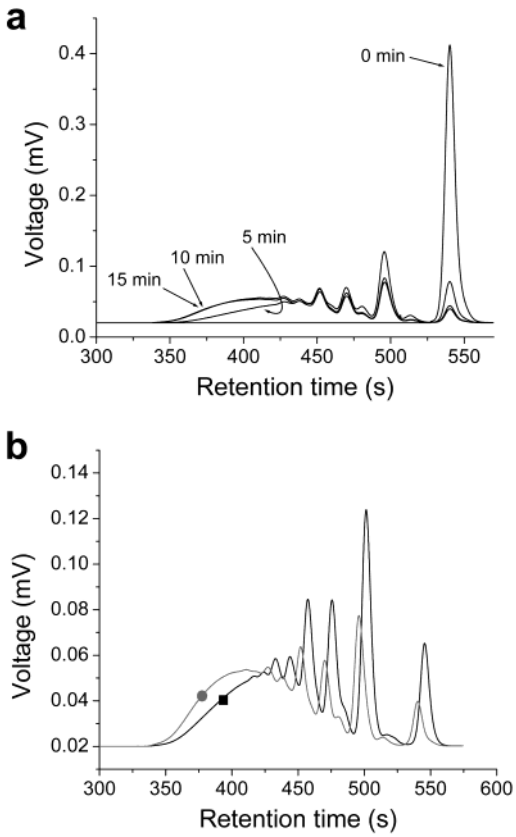

Figure 3. Size exclusion chromatograms of 5% w/w solutions in chloroform at 25 °C, containing 1% w/w photoinitiator, of (a) **ThE 6b6**, exposed to UV-irradiation for the indicated periods of time. (b) **ThE 6b4** (■) and **ThE 6b6** (●), both photopolymerized for 15 min.

Figure 3a presents the photoinitiated polymerization of 5% w/w **ThE 6b6** in chloroform at 25 °C for several distinct irradiation times. Polymerization occurs to a reasonable degree, but it appears that the ultimate degree of polymerization in

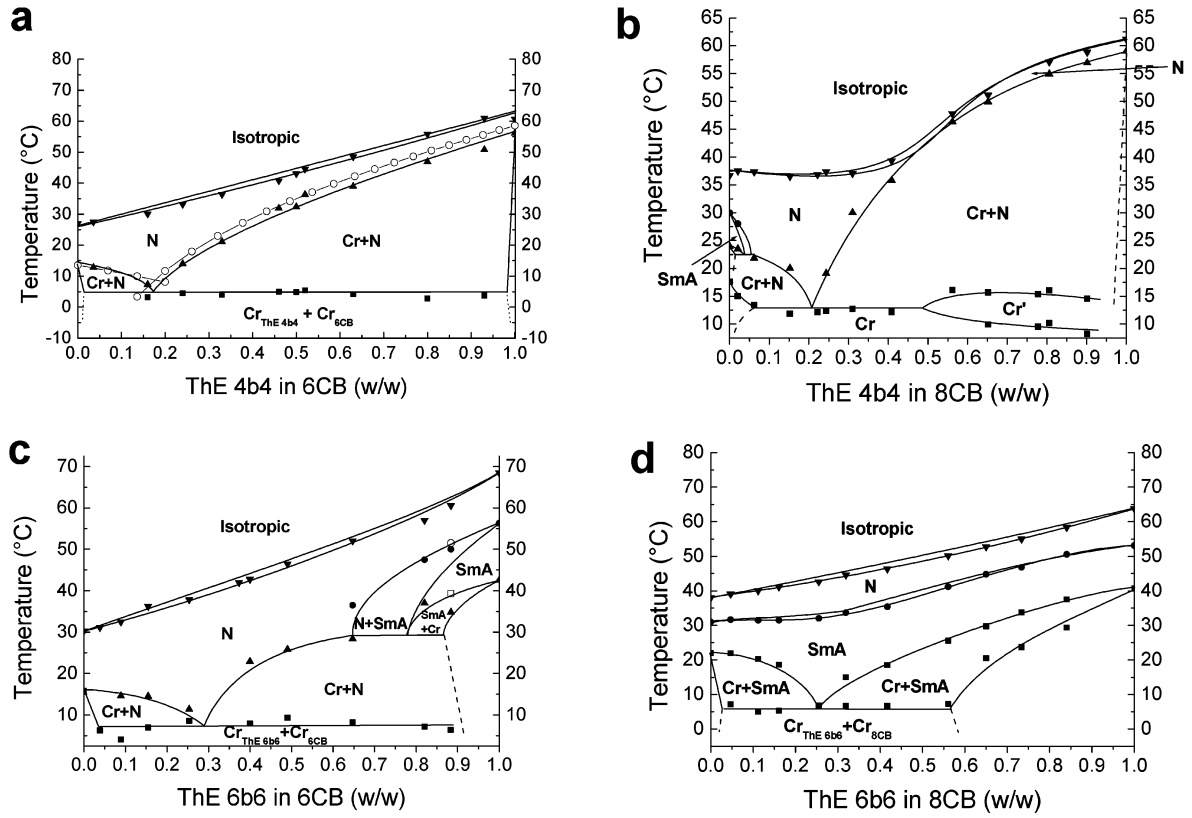

Figure 4. Phase diagrams of combinations of the liquid crystalline thiol-ene monomers **ThE 4b4** and **ThE 6b6** with the cyanobiphenyls **6CB** and **8CB**. (a) **ThE 4b4** + **6CB**. The open circles -○- indicate the calculated liquidus. (b) **ThE 4b4** + **8CB**. (c) **ThE 6b6** + **6CB**. (d) **ThE 6b6** + **8CB**.

chloroform is obtained after approximately 10 min, as hardly any increase in molecular weight is noticed when the molecular weight distributions corresponding to irradiation times of 10 and 15 min are compared. It should be noted, however, that chloroform can play a role in free-radical propagated polymerizations, by acting as a transfer agent, as is common in acrylate polymerizations, for instance.[26] A similar situation may be valid for 4-chloroanisole. The solubility of the resulting polymer in the solvent will also play a role. When the experiments were repeated at 60 °C, no noticeable increase in monomer conversion was observed. This could well be related to the influence of the temperature on the position of the equilibrium of the rate-determining step in the thiol-ene addition reaction (Scheme 1-II).

A comparison between the polymerization behavior of the monomers **ThE 6b6** and **ThE 6b4** after polymerization for 15 min is made in Figure 3b, where the residual monomer and oligomeric fractions can be distinguished. Under the same polymerization conditions for both monomers, a larger degree of polymerization is observed for **ThE 6b6** compared to its analogue **ThE 6b4**. This indicates that the larger flexibility in the aliphatic chain of **ThE 6b6**, resulting from its larger spacer length, favors polymerization.

Phase Diagrams. To generate the main-chain liquid crystalline thiol-ene polymers in anisotropic solvents, by using photoinitiation of aligned monomers, an initial situation is required where both monomer and anisotropic solvent form a homogeneous mixture. The commercially available cyanobiphenyls are ideal candidates for the role of the anisotropic solvent, as they display low melting temperatures and exhibit a variety of mesophases that can be tuned by the appropriate choice of the spacer length. Figure 4a−d shows binary phase diagrams, obtained upon mixing the thiol-ene monomers **ThE 4b4** and **ThE 6b6** with either of the cyanobiphenyls **6CB** or **8CB**. In each case, the pure materials display either a single nematic phase or a nematic and a smectic A phase, depending on the temperature. The binary phase diagrams were obtained by combining DSC, polarized optical microscopy and occasionally wide-angle X-ray spectroscopy. To approximate thermodynamic equilibrium more closely, the transitions were determined in heating mode at slow speeds, thus avoiding supercooling effects that can frequently be found in cooling mode.

Figure 4a, showing the miscibility behavior of **ThE 4b4** and **6CB**, depicts the typical eutectic phase diagram that is obtained when two miscible nematic materials are mixed. The eutecticum is found at 17.3% w/w **ThE 4b4**, resulting in a melt transition that is substantially lower than that of the pure compounds separately. It is also possible to calculate the melting curves (liquidus) and the eutecticum, as shown by Demus et al.[27] On the basis of certain assumptions, such as the occurrence of an ideally mixed liquid phase and the absence of the formation of mixed crystals upon crystallization, they were able to derive the relationship between the upper melting temperature T_i of the crystalline-nematic two-phase region and the concentration x_i of one of the components in the binary system:

$$T_i = \frac{\Delta H_{oi}}{\frac{\Delta H_{oi}}{T_{oi}} - R \ln x_i} \qquad (1)$$

where ΔH_{oi} is the molar heat of fusion, T_{oi} is the melting point, and x_i is the mole fraction, all of component i, whereas R is the gas constant. The construction of the intersection of the temperature-mole fraction curves (using 31.8 and 20.1 kJ mol^{-1} for the molar heats of fusion of **ThE 4b4** and **6CB**, respectively, and using 331.8 and 286.7 K for the respective melting points) results in the calculated eutecticum at T = 8.6 °C and 17.4% w/w **ThE 4b4** (see the open circles -○- in Figure 4a). Both

values are in close approximation with the experimental values (5.1 °C; 17.3% w/w), confirming the almost ideal mixing behavior of the two components.

The two-phase regions in this phase diagram enclose a homogeneous nematic phase region that exists at ambient temperatures over the entire concentration composition. The nematic to isotropic transition shows a linear dependency on the concentration, indicating the perfect interaction between the two components on a molecular level. Combined with the melting point depression because of the eutectic behavior, the resulting nematic existence gap is extended when compared to the nematic phase existence of the two individual components separately.

The ideal miscibility behavior as observed for the **ThE 4b4/6CB** combination is certainly not observed when the 6-spacered cyanobiphenyl is replaced by its 8-spacered homologue, **8CB** (Figure 4b). In essence, the eutectic behavior is observed again, combined with a crystal−crystal transition region, but the unsymmetrical nematic to isotropic transition curve already suggests the less perfect molecular interaction between the thiol-ene monomer and the anisotropic solvent. Moreover, the occurrence of the smectic A phase, originating from **8CB**, is almost immediately extinguished when the monomer concentration is increased, also indicating the less well-defined miscibility behavior between the two components. In addition, although a homogeneous nematic phase is noticeable over the entire concentration composition, its existence gap is almost diminished at a 1:1 monomer-solvent ratio. The increased difference of the spacer lengths is apparently responsible for a less favorable packing of the two components in the liquid crystalline phase.

In turn, replacing the **ThE 4b4** monomer with its **ThE 6b6** counterpart and mixing it with **6CB** results in the diagram shown in Figure 4c. A homogeneous nematic phase is again obtained that extends over the entire concentration gradient. The smectic A phase, originating from **ThE 6b6**, extends slightly into the phase diagram, although the real situation in the smectic A region may differ slightly from that depicted in Figure 4c, as the depicted course is an estimation based on only a few observations.

The binary phase diagram of **ThE 6b6** and **8CB** (Figure 4d) contains both a homogeneous nematic phase and a smectic A phase over the entire concentration gradient. The two mesophase regions are again accessible at ambient temperatures.

From the four binary phase diagrams, we can infer that all combinations of thiol-ene monomers and cyanobiphenyls result in homogeneous mesophases over the entire concentration gradient, accessible at ambient temperatures. The type of mesophase can be varied between a nematic phase and a smectic A phase, depending on the choice of the combination of the thiol-ene monomer and the cyanobiphenyl solvent. The **ThE 4b4/6CB** (Figure 4a) and the **ThE 6b6/8CB** (Figure 4d) combinations are particularly useful mixtures because of their widely extended nematic and/or smectic phase, for each monomer/solvent ratio. These liquid crystalline thiol-ene/ cyanobiphenyl combinations form unique reactive room-temperature LC mixtures with variable mesophases.

Polymerization in Anisotropic Solvents. Having established the miscibility behavior of the thiol-ene monomers with inert anisotropic solvents, the ability of these monomers to polymerize in their anisotropic environment was investigated. Figure 5 shows an SEC chromatogram for a 25% w/w mixture of **ThE 4b4** in **6CB**, containing 1% w/w photoinitiator, based on the monomer. From the corresponding phase diagram, Figure 4a, we can infer that this mixture exhibits a nematic phase at the polymerization temperature of 25 °C. Strictly speaking, this mixture is not a binary mixture but a ternary mixture, because it contains a third component, the photoinitiator. However, because of the minute amount of this component (1% w/w based on the monomer), it is assumed that the addition of this component has no noticeable influence on the phase behavior and phase transition temperatures of the binary mixture, and consequently, the mixture is treated as a binary mixture. This assumption was checked on several occasions, and shifts in the clearing point were roughly 0.5 °C for a mixture containing 1% w/w photoinitiator in comparison to the true binary mixture containing no initiator.

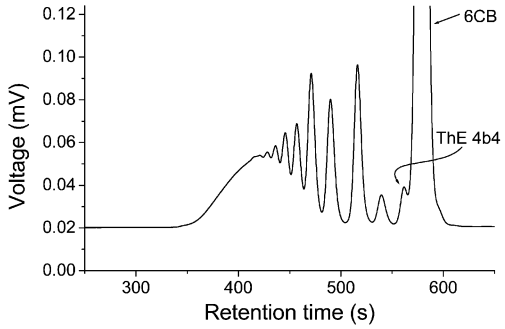

Figure 5. Size exclusion chromatogram of 25% w/w **ThE 4b4** in **6CB**, photopolymerized for 25 min at 25 °C, using a 1% w/w photoinitiator concentration.

The SEC analysis shows that in an anisotropic environment, i.e., in the cyanobiphenyl **6CB**, polymerization also occurs to a substantial degree, shown here for the situation after 25 min at 25 °C. The chromatogram shows a large signal (578 s, intensity off-scale) belonging to the residual solvent **6CB**, next to the signals of the monomer (562 s), oligomeric species (i.e. dimer, trimer, etc.), and polymeric fractions ($\bar{M}_n$ =5.8 kg mol^{-1}).

Kinetic Evaluation. A quantitative analysis of the photoinitiated bulk polymerization kinetics of the thiol-ene monomers, using time-resolved Raman spectroscopy, has been reported previously.[22] Because the polymerizations in anisotropic solvents are performed in solution rather than in bulk, the spectral bands of reactive groups in the monomer are no longer detected using Raman spectroscopy. Nuclear magnetic resonance (NMR) is an alternative, but it has the disadvantage that for a reliable determination of the conversion, for instance, all higher molecular weight fractions require dissolution. NMR is also not the first choice if we take into account the aforementioned solubility difficulties involving the polymerization experiments in isotropic solvents, and the relatively high concentrations required (3−10 mg mL^{-1}) for an acceptable signal-to-noise ratio in a reasonable time span. Conversely, SEC offers the benefit of requiring lower sample concentrations, e.g. 0.1 mg mL^{-1}.

The determination of the overall conversion can be based on two calculations. One approach is to compare the area of the residual monomer peak to the total area of the chromatogram.[25] However, this also requires a completely dissolved sample, including the higher molecular weight fractions. Because of the UV-detection method used in the SEC analysis, it is furthermore assumed that the extinction coefficients of the higher molecular weight species do not differ from that of the monomer. This assumption seems reasonable because the only difference between the chromophores of the monomer and the oligomers/polymers is the disappearance of the carbon−carbon double bond and the replacement of the thiol group by a sulfide group.

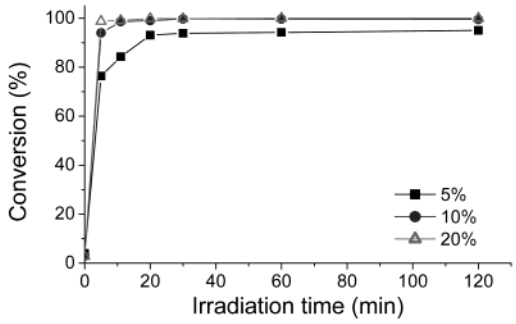

Figure 6. Overall conversion, determined using SEC, of **ThE 4b4** solutions in **6CB**, photopolymerized at 30 °C for distinct irradiation times and concentrations. The photoinitiator concentration is 1% w/w, based on the monomer.

Usually, the excitation bands for the (n,π*) transition and (n,σ*) transition of these isolated chromophores are located at wavelengths below 200 nm and around 235 nm,[28] respectively, much lower than the wavelength of 263 nm used for detection during the analysis.

A second approach is based on the comparison between the monomer peak area at time t and the monomer peak area before polymerization ($t = 0$). Provided both samples have a known concentration in the eluent used for analysis, it is not necessary for the higher molecular weight fractions to dissolve completely for determination of the conversion, as long as the residual monomer is completely dissolved. This seems certainly most likely at the low concentrations used for analysis.

The overall conversion at 30 °C is shown in Figure 6 for several concentrations of the thiol-ene monomer **ThE 4b4** in **6CB**.

Similar to the results seen for polymerization in isotropic solvents and indicated by the SEC trace in Figure 5, a high degree of polymerization is obtained when a thiol-ene monomer is polymerized in an anisotropic solvent, as indicated by the high overall conversions after prolonged irradiation. The usual monomer concentration/conversion relationship is observed where a higher monomer content results in a higher polymerization rate, indicated by the increasing steepness of the curves for higher monomer percentages. A higher ultimate overall conversion is also obtained for higher monomer concentrations. In Figure 7, a comparison is made for two monomer concentrations at different polymerization temperatures.

The overall polymerization rate noticeably decreases with increasing temperature. This reflects the influence of the temperature on the equilibrium position of the rate-determining step of the thiol-ene addition reaction (Scheme 1-II). The backward reaction becomes more important as the temperature increases, because its rate constant is more temperature dependent than the rate constant for the forward reaction, because of the usually higher activation energy of the backward reaction.[29−31] Consequently, the net rate of polymerization decreases until it falls to zero at the ceiling temperature T_c. This effect may become more pronounced with lower monomer concentrations, similar to the situation for addition polymerizations, where the ceiling temperature is generally lowered with decreasing monomer concentrations.[32] This may explain why the ceiling temperature effect is not yet experienced for bulk polymerizations of **ThE 4b4** but is more pronounced for polymerizations of **ThE 4b4** in solution, as shown here.[22,33]

Higher conversions at lower temperatures are actually advantageous, as they do not limit the use of the thiol-ene/anisotropic solvent mixtures, as outlined by their phase diagrams.

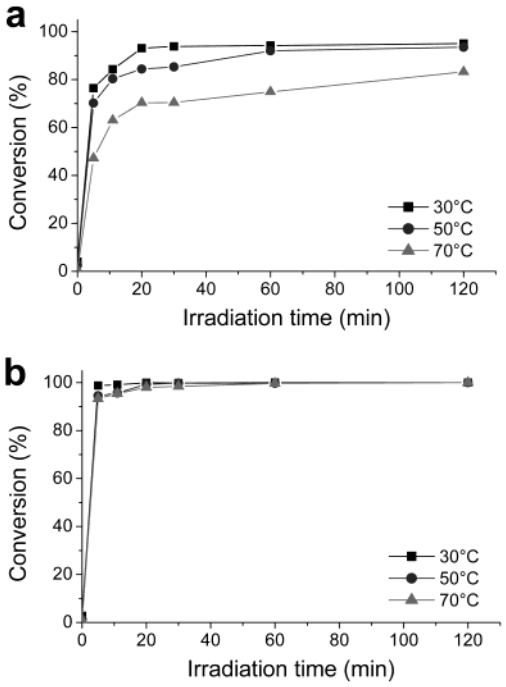

Figure 7. Overall conversion, determined using SEC, of **ThE 4b4** solutions in **6CB**, photopolymerized at the indicated temperatures and irradiation times. The photoinitiator concentration is 1% w/w, based on the monomer. (a) 5% w/w monomer. (b) 20% w/w monomer.

After all, higher polymerization temperatures would imply the polymerization of thiol-ene monomers proceeding in the isotropic phase, whereas the objective is to make use of the molecular organization that is only available at ambient temperatures.

Morphological Evaluation. For the in situ photogeneration of the discussed morphologies, an initially homogeneous phase is required, consisting of both monomer and inert anisotropic solvents; suitable mixtures were introduced earlier in Figure 4a,d. However, these phase diagrams will change immediately upon polymerization. As soon as oligomeric species are formed, phase separation sets in, as the solubility of liquid crystalline polymers is generally not very good in LC solvents, which is due to the only small increase of the entropy term of the free energy of mixing.[34,35] However, phase separation is actually essential for the creation of the desired linear polymeric structures. The key factor in the polymerization process is the control of the resulting morphology. Specifically, it is desirable to engineer the morphology both on a macroscopic scale and on a nanoscopic scale. For this reason, planarly oriented nematic mixtures of **ThE 4b4** and **6CB**, containing 1% w/w photoinitiator, were subjected to UV-irradiation, and the resulting morphology was investigated using optical microscopy and SEM (Figure 8). The architectures found and depicted here are representative for all monomer concentrations investigated, in the range from 5 to 40% w/w **ThE 4b4**. Because the micrographs were obtained after extraction of the low molecular weight components (e.g., solvent and residual monomer, see the Experimental Section), the remnants in the micrographs correspond to the polymeric fragments that were formed during the polymerization process.

From Figure 8, we can clearly infer that linear structures, defined here as type I structures, have resulted from the polymerization process, as intended. On average, a preferred direction for these type I structures is noticeable, which coincides with the rubbing direction of the polyimide alignment layer used

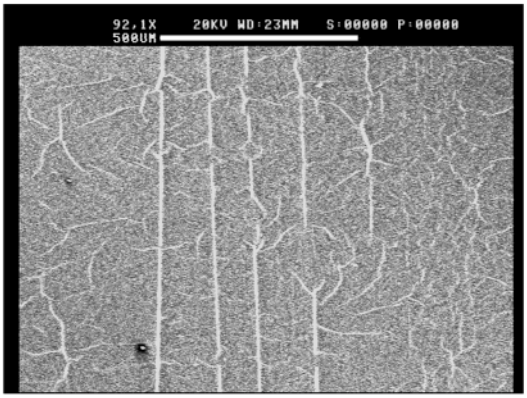

a

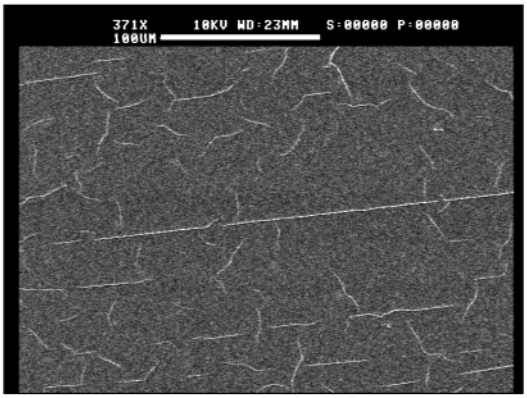

b

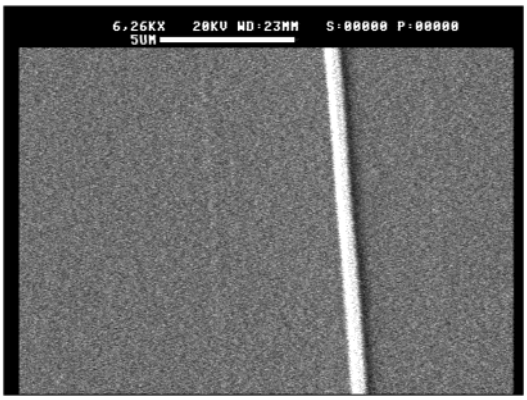

c

Figure 8. Scanning electron micrographs showing Type I structures obtained from photopolymerized (>70 min) **ThE 4b4/6CB** mixtures in an initially planarly oriented nematic phase containing 1% w/w photoinitiator. (a) 20% w/w **ThE 4b4** (scale bar 500 μm, rubbing direction up−down). (b) 40% w/w **ThE 4b4** (scale bar 100 μm, rubbing direction left-to-right). (c) Detail (scale bar 5 μm) of micrograph shown in a.

to align the mesophase. Deviations from the preferred direction can be observed. The scattering present in the predominant direction of the polymeric fiberlike structures is probably related to director fluctuations present in the nematic mesophase. Upon closer inspection, we can also identify occasional threads that branch off from the main structure at an approximate angle of 75°. This points toward the incorporation of defects during the polymerization process. Similar observations have been made for the crystallization of α-polypropylene, where 99° microbranching is occasionally observed.[36]

Based on the dimensions inferred from the electron micrographs, e.g., a diameter of approximately 800 nm, the threadlike architectures cannot simply be single polymer chains, because these would be impossible to see using SEM and must therefore consist of aggregates of polymer chains. However, attempts to isolate the threadlike architectures, to investigate their properties, failed. Consequently, the internal structure, i.e., the alignment of the mesogens, the degree of order, etc., of these structures is as yet unresolved. However, it will be clear from Figure 8a, for instance, that if the initial orientation of the liquid crystal mixture is chosen perpendicular to the substrate's surface, the obtained fibril lengths (>0.5 mm) can potentially exceed typical cell-gaps used for device construction (5−20 μm) several times.

The picture sketched here is not yet complete, however. Irrespective of the polymerization conditions, all samples also predominantly show different type II structures, as shown in Figure 9.

These type II structures are undesirable, because the overall degree of order is decreased and the uncontrollable size and position of the structures causes the absorption and scattering of light on a large scale. These dendritic "cauliflower" structures appear to originate from an involved nucleation and aggregation mechanism during the polymerization process, which was confirmed by optical microscope observations. Differential scanning calorimetry measurements already showed that the pure polymers are semicrystalline materials,[22] and these findings are in agreement with X-ray measurements of a crystalline thiol-ene polymer obtained from bulk polymerization, shown in Figure 10, and of a thiol-ene monomer/anisotropic solvent mixture, before and after polymerization. The diffraction pattern of the mixture is predominantly determined by the nematic cyanobiphenyl and, to a lesser extent, by the semicrystalline structures. Yet, the superposition of the diffraction pattern of the pure polymer is clearly visible, taking into account that the diffraction patterns were measured at different temperatures, confirming the semicrystalline character of the polymeric structures in the mixture.

Crystallization processes are involved in the morphology development during the in situ photopolymerization of the thiol-ene/cyanobiphenyl mixtures used here. These crystallization processes are not detrimental by themselves, as long as they occur in a controlled, ordered fashion, leading to type I structures as seen earlier, for instance. Unfortunately, this is certainly not the case for the situations outlined here. The balance between the type I and type II structures needs to be shifted in favor of the threadlike type I structures. If the enforced growth of the polymer chains, imposed by the molecular organization, can be increased to exceed the rate of crystallization, linear type I structures may result. Using this kinetic approach, the length of the forming oligomer/polymer chains becomes sufficiently large, causing the chain mobility to decrease to such an extent that the time required for rearrangement and folding of the polymer chains necessary for the formation of type II structures is insufficient compared to the growth of the polymer chains themselves.

Polymerizations performed with variable photoinitiator concentrations in the range 0.5−5% w/w, based on the monomer, were however unsuccessful in shifting the morphological balance.[23] An increase of the radical flux effectuated through an increased UV-light intensity or through the use of electron beam initiation resulted in the expected increased overall

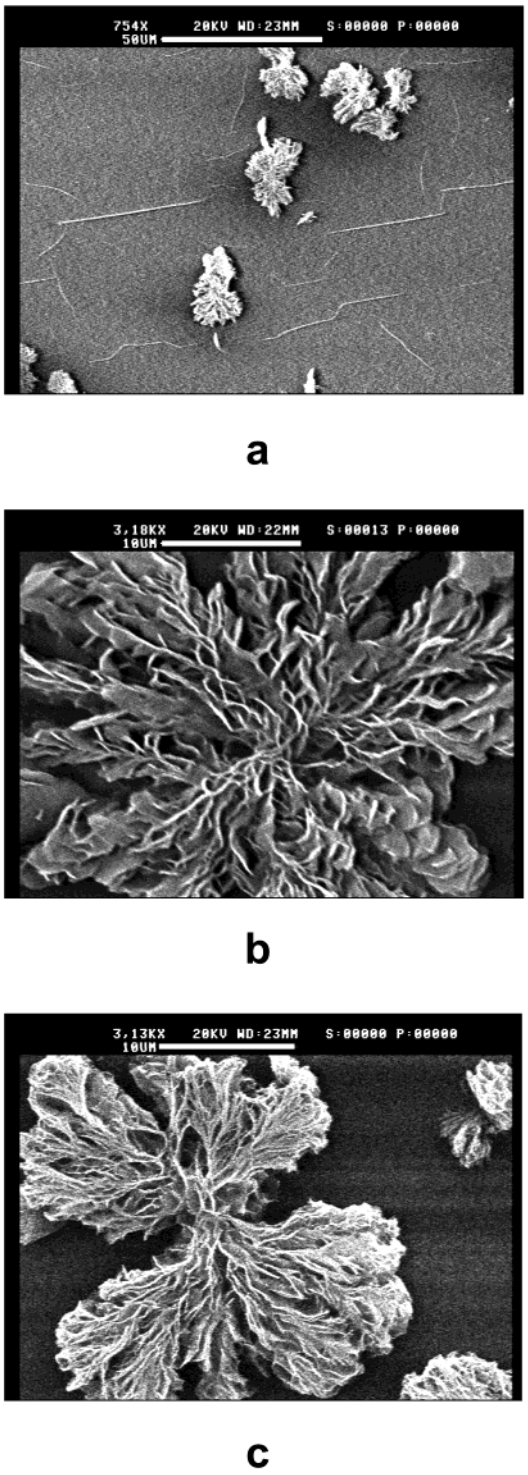

Figure 9. Scanning electron micrographs showing type II structures typically obtained from photopolymerized thiol-ene monomers in anisotropic media. (a) Combination of type I and type II structures, here shown for an initially planarly oriented 10% w/w **ThE 4b4/6CB** mixture (scale bar 50 μm). (b) Magnification of a type II "cauliflower" structure (scale bar 10 μm). (c) Selected type II structure (scale bar 10 μm).

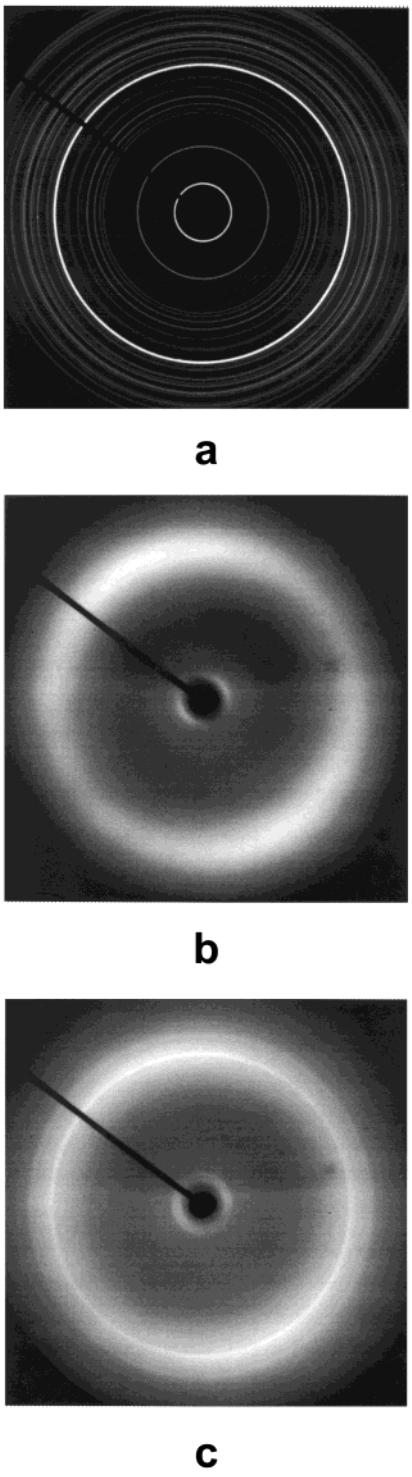

Figure 10. X-ray diffraction patterns of (a) **Poly(ThE 4b4)** at 80 °C, photopolymerized in bulk at 150 °C. (b) 5% w/w **ThE 4b4** in **6CB** at 25 °C, before polymerization. (c) System shown in b, after photopolymerization at 25 °C.

reaction rate, but crystallization, predominantly of type II structures, was still observed.[23]

The morphology may also be controlled further using a thermodynamic approach. One of the critical moments during the polymerization process is the onset of phase separation. From that point on, either type I or type II structures will be formed. If the onset of phase separation could be delayed, the growing polymer chains would remain in solution for a longer period of time, and the length of the growing polymer chain would therefore increase. The probability of rearrangement and folding of the polymer chains in type II structures would also decrease because of the reduced mobility of the longer polymer chains. For this approach, the use of different monomers that resemble the chemical structure of the cyanobiphenyl solvent used here (e.g., biphenyl based thiol-enes)[21] or the use of different monomer/solvent combinations, is required.

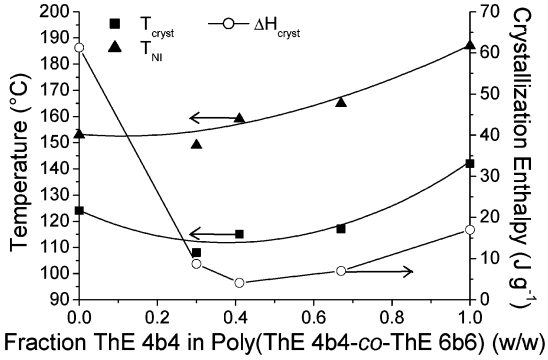

Figure 11. Nematic-to-isotropic transition temperature, crystallization temperature and crystallization enthalpy of different **Poly(ThE 4b4-*co*-ThE 6b6)** copolymer compositions (w/w).

Irrespective of the use of the discussed kinetic or thermodynamic approach, the major concern appears to be the intrinsic crystallization behavior of the thiol-ene polymers. Random copolymerization can be an effective way to lower the crystal-to-mesophase transition temperature of liquid crystalline copolymers and to extend the mesophase temperature range with respect to the corresponding homopolymers. The effect increases when the difference in length of the flexible spacers of the comonomers increases.[37] In this way, it may be feasible to lower the melt and crystallization temperature, thereby lowering the driving force for crystallization of the copolymers or to suppress the crystallization of the liquid crystalline thiol-ene copolymers as a whole.

Figure 11 shows the nematic-to-isotropic transition temperature, the crystallization temperature, and crystallization enthalpy of copolymers synthesized from **ThE 4b4** and **ThE 6b6**. There is a noticeable decrease of the crystallization enthalpy, with a minimum enthalpy at an approximate 50/50 w/w **ThE 4b4** fraction, indicating the positive effect of copolymerization on the reduction of the crystallization tendency of the copolymer compared to the corresponding homopolymers. The crystallization enthalpies did not increase significantly when the samples were measured again after being stored for one week at ambient temperature. However, the tendency for crystallization is not completely diminished. Alternatively, copolymerization using monomers with spacers with comparable length but different parity can decrease the tendency for crystallization even further, as it negatively affects the packing requirements of the solid state of the copolymer. A decrease of the crystallization enthalpy was also observed for a **Poly(ThE 4b4-*co*-ThE 5b4)** copolymer in comparison to the two corresponding homopolymers, but crystallization was nevertheless not eliminated despite the different parity of the spacers of the comonomers.

Finally, crystallization can also be suppressed by the formation of copolymers comprised of monomers with different mesogenic cores, combining for instance phenyl benzoate-based thiol-ene monomers and biphenyl-based thiol-ene monomers.[21] However, important considerations are the required initially homogeneous mesophase and the possibility of composition drift during polymerization, which may result in microphase separation and possible crystallization.

Conclusions

In this paper, we show that phenyl benzoate-based liquid crystalline thiol-ene monomers can be photopolymerized to a substantial degree, both in isotropic and anisotropic solvents. Upon mixing of the thiol-ene monomers with inert anisotropic solvents, i.e., cyanobiphenyls, unique reactive liquid crystalline mixtures are obtained that exhibit variable mesophases at ambient temperatures, depending on the correct combination of monomer and solvent. Indications for the occurrence of a ceiling temperature effect, commonly found in conventional addition polymerizations, were also observed for the free-radical propagated step-growth thiol-ene polymerization. The effect was more pronounced for higher polymerization temperatures and for lower initial monomer concentrations, similar to the situation encountered in conventional addition polymerizations.

The in situ photopolymerization of the thiol-ene monomers in anisotropic solvents can lead to the formation of linear, threadlike architectures. However, complex morphological changes occur during the polymerization process, and crystallization processes are involved that induce the formation of uncontrolled, dendritic crystalline structures. Several approaches directed toward the elimination of the uncontrolled crystalline structures in favor of the linear structures have been presented here. Kinetic and thermodynamic approaches did not result in the intended morphological shift. Copolymerization experiments were conducted to diminish the intrinsic tendency for crystallization of the formed thiol-ene polymers.

The studied principles for self-organization and enforced organization have successfully led to the partial formation of intriguing threadlike architectures, in combination with not yet fully controlled fractal-like structures. This is a stimulant for further research into the optimization of morphology control during the in situ polymerization of liquid crystalline thiol-ene monomers and may ultimately open new possibilities in the design, manufacturing, and application of electrooptical devices.

References and Notes

(1) Friend, R. H.; Gymer, R. W.; Holmes, A. B.; Burroughes, J. H.; Marks, R. N.; Taliani, C.; Bradley, D. D. C.; Dos Santos, D. A.; Brédas, J. L.; Lögdlund, M.; Salaneck, W. R. *Nature* **1999**, *397*, 121−128.

(2) Grätzel, M. *Nature* **2001**, *409*, 575−576.

(3) Fergason, J. L. *SID Dig. Technol. Pap.* **1985**, *16*, 68−70.

(4) Van Boxtel, M. C. W.; Janssen, R. H. C.; Broer, D. J.; Wilderbeek, H. T. A.; Bastiaansen, C. W. M. *Adv. Mater.* **2000**, *12*, 753−757.

(5) Coles, H. J. *J. Chem. Soc., Faraday Discuss.* **1985**, *79*, 201−214.

(6) Hikmet, R. A. M. *J. Appl. Phys.* **1990**, *68*, 4406−4412.

(7) Drzaic, P. S. *Liquid Crystal Dispersions*; World Scientific: Singapore, 1995.

(8) Wilderbeek, H.; De Koning, H.; Vorstenbosch, J.; Chlon, C.; Bastiaansen, K.; Broer, D. J. *Jpn. J. Appl. Phys., Part 1* **2002**, *41*, 2128−2138.

(9) Penterman, R.; Klink, S. I.; De Koning, H.; Nisato, G.; Broer, D. J. *Nature* **2002**, *417*, 55−58.

(10) Chien, L.-C.; Boyden, M. N.; Walz, A. J.; Shenouda, I. G.; Citano, C. M. *Mol. Cryst. Liq. Cryst.* **1998**, *317*, 273−285.

(11) Roganova, Z. A.; Zmolyansky, A. L.; Kostromin, S. G.; Shibaev, V. P. *Eur. Polym. J.* **1985**, *21*, 645−650.

(12) Lub, J.; Broer, D. J.; Van den Broek, N. *Liebigs Ann./Recueil* **1997**, (*11*), 2281−2288.

(13) Lub, J.; Broer, D. J.; Martinez Antonio, M. E.; Mol, G. N. *Liq. Cryst.* **1997**, *24*, 375−379.

(14) Fukumasa, M.; Takeuchi, K.; Kato, T. *Liq. Cryst.* **1998**, *24*, 325−327.

(15) Kato, T.; Kutsuna, T.; Hanabusa, K.; Ukon, M. *Adv. Mater.* **1998**, *10*, 606−608.

(16) Mizoshita, N.; Kutsuna, T.; Hanabusa, K.; Kato, T. *Chem. Commun.* **1999**, 781−782.

(17) Jacobine, A. F. In *Radiation Curing in Polymer Science and Technology*; Fouassier, J. P., Rabek, J. F., Eds.; Elsevier Applied Science: London, 1993; Vol. 3, Chapter 7.

(18) Wilderbeek, H. T. A.; Van der Meer, F. J. A.; Feldman, K.; Broer, D. J.; Bastiaansen, C. W. M. *Adv. Mater.* **2002**, *14*, 655−658.

(19) Galli, G.; Chiellini, E.; Angeloni, A. S.; Laus, M. *Macromolecules* **1989**, *22*, 1120−1124.

(20) Lub, J.; Broer, D. J.; Allan, J. F. *Mol. Cryst. Liq. Cryst.* **1999**, *332*, 259−266.

(21) Wilderbeek, H. T. A.; Van der Meer, M. G. M.; Jansen, M. A. G.; Nelissen, L.; Fischer, H. R.; Van Es, J. J. G. S.; Bastiaansen, C. W. M.; Lub, J.; Broer, D. J. *Liq. Cryst.* **2002**, in press.

(22) Wilderbeek, H. T. A.; Goossens, J. G. P.; Bastiaansen, C. W. M.; Broer, D. J. *Macromolecules* **2002**, *35*, 8962−8968.

(23) Wilderbeek, H. Ph.D. Thesis, Eindhoven University of Technology, Eindhoven, The Netherlands, 2001; ISBN 90-386-2972-9.

(24) Yang, D.-K.; Chien, L.-C.; Fung, Y. K. In *Liquid Crystals in Complex Geometries. Formed by polymer and porous networks*; Crawford, G. P., Zumer, S., Eds.; Taylor & Francis: London, 1996; Chapter 5.

(25) Ogiri, S.; Kanazawa, A.; Shiono, T.; Ikeda, T.; Nishiyama, I.; Goodby, J. W. *Macromolecules* **1998**, *31*, 1728−1734.

(26) Raghuram, P. V. T.; Nandi, U. S. *J. Polym. Sci., Part A-1* **1970**, *8*, 3079−3088.

(27) Demus, D.; Fietkau, C.; Schubert, R.; Kehlen, H. *Mol. Cryst. Liq. Cryst.* **1974**, *25*, 215−232.

(28) Hesse, M.; Meier, H.; Zeeh, B. *Spektroskopische Methoden in der organischen Chemie*; Georg Thieme Verlag: Stuttgart, Germany, 1995.

(29) Sawada, H. In *Thermodynamics of Polymerisation*; O'Driscoll, K. F., Ed.; Marcel Dekker Inc.: New York, 1976; Chapter 1.

(30) Pallen, R. H.; Sivertz, C. *Can. J. Chem.* **1957**, *35*, 723−733.

(31) Sivertz, C. *J. Phys. Chem.* **1959**, *63*, 34−38.

(32) Ivin, K. J. *J. Polym. Sci., Part A*: *Polym. Chem.* **2000**, *38*, 2137−2146.

(33) For an estimated monomer density of 1.3 g mL^{-1}, a bulk monomer concentration of approximately 3.5 M can be calculated. The monomer concentration used in anisotropic solutions is approximately 0.15−0.30 M. The monomer density is estimated using the additive group contributions approximation by Van Krevelen, D. W. *Properties of Polymers*, 3rd ed.; Elsevier: Amsterdam, 1990.

(34) Papkov, S. P. *Adv. Polym. Sci.* **1983**, *59*, 75−102.

(35) Koningsveld, R.; Stockmayer, W. H.; Nies, E. *Polymer Phase Diagrams*; Oxford University Press: Oxford, U.K., 2001.

(36) Lovinger, A. J. *J. Polym. Sci.*: *Polym. Phys. Ed.* **1983**, *21*, 97−110.

(37) Chiellini, E.; Laus, M. In *Handbook of Liquid Crystals*; Demus, D., Goodby, J. W., Gray, G. W., Spiess, H.-W., Vill, V., Eds.; Wiley-VCH: Weinheim, Germany, 1998; Vol. 3, Chapter 2.